Published in final edited form as:
Biochemistry. 2013 July 30; 52(30): 5125–5132. doi:10.1021/bi4002985.

Redesign of substrate specificity and identification of aminoglycoside binding residues of Eis from *Mycobacterium tuberculosis*

Benjamin C. Jennings[a,§], **Kristin J. Labby**[a,§], **Keith D. Green**[b], and **Sylvie Garneau-Tsodikova**[b,*]

[a]Life Sciences Institute, 210 Washtenaw Avenue, University of Michigan, Ann Arbor, MI 48109-2216, United States

[b]Department of Pharmaceutical Sciences, University of Kentucky, Lexington, KY 40536-0596, United States

Abstract

The upsurge of drug-resistant tuberculosis (TB) is an emerging global problem. Increased expression of the enhanced intracellular survival (Eis) protein is responsible for clinical resistance to aminoglycoside (AG) antibiotics in *Mycobacterium tuberculosis*. Eis from *M. tuberculosis* (Eis_*Mtb*) and from *M. smegmatis* (Eis_*Msm*) both function as acetyltransferases capable of acetylating multiple amines of many AGs; however, these Eis homologs differ in AG substrate preference and number of acetylated amine groups per AG. The AG binding cavity of Eis_*Mtb* is divided into two narrow channels, whereas Eis_*Msm* contains one large cavity. Five bulky residues lining one of the AG binding channels of Eis_*Mtb*, His119, Ile268, Trp289, Gln291, and Glu401, have significantly smaller counterparts in Eis_*Msm*, Thr119, Gly266, Ala287, Ala289, and Gly401, respectively. To identify the residue(s) responsible for AG binding in Eis_*Mtb* and functional differences from Eis_*Msm*, we have generated single, double, triple, quadruple, and quintuple mutants of these residues in Eis_*Mtb* into their Eis_*Msm* counterparts and tested their acetylation activity with three structurally diverse AGs: kanamycin A (KAN), paromomyin (PAR), and apramycin (APR). We show that the penultimate C-terminal residue Glu401 plays a critical role in the overall activity of Eis_*Mtb*. We also demonstrate that the identities of residues Ile268, Trp289, and Gln291 (in Eis_*Mtb* nomenclature) dictate the differences between acetylation efficiencies of Eis_*Mtb* and Eis_*Msm* for KAN and PAR. Finally, we show that the mutation of Trp289 in Eis_*Mtb* into Ala plays a role in APR acetylation.

Keywords

Acetyltransferase; Aminoglycoside antibiotics; Enhanced intracellular survival protein; Site-directed mutagenesis; Resistance

[*]**Corresponding Author:**sylviegtsodikova@uky.edu; Phone: (859) 218-1686; Fax: (859) 257-7585.
[§]These authors contributed equally to this work.

The authors declare no competing financial interest.

ASSOCIATED CONTENT

Supporting Information includes: a table of the primers used in this study (Table S1), a table of the primer combinations and templates used to construct the Eis_*Mtb*-mutants (Table S2), a table of the purification yields of the Eis_*Mtb*-mutants (Table S3), a figure of an SDS-PAGE gel showing all of the Ni^{II}-NTA-purified proteins used in this study (Figure S1), kinetic curves of the Eis_*Mtb*-mutants with AGs (Figure S2–S4), representative mass spectra of PAR acetylation by Eis_*Mtb*, Eis_*Msm*, and Eis_*Mtb*-mutants (Figure S5), and representative TLC time course of KAN di-acetylation by Eis_*Mtb*, Eis_*Msm*, and Eis_*Mtb*-mutants (Figure S6). This material is available free of charge via the Internet at http://pubs.acs.org.

Aminoglycosides (AGs) (Figure 1A) are broad-spectrum antibiotics used to treat many serious bacterial infections including multidrug-resistant (MDR) and extensively drug-resistant (XDR) tuberculosis (TB). Resistance to AGs is increasing, leading to higher numbers of cases of extremely and totally drug-resistant TB.[1–3] In *Mycobacterium tuberculosis* (*Mtb*), upregulation of the enhanced intracellular survival (*eis*) gene is responsible for resistance to the second-line anti-TB drugs kanamycin A (KAN, Figure 1A) and amikacin.[4–6] The Eis protein is an acetyltransferase that efficiently acetylates AGs, thereby inactivating them as antibiotics.[4, 7]

Mtb and the homologous non-pathogenic model mycobacterium *M. smegmatis* (*Msm*) share many (>2,000) protein homologs including virulence genes and maintain the same unusual cell wall structure.[8] We previously reported that Eis from *Mtb* (Eis_*Mtb*) and *Msm* (Eis_*Msm*) are acetyl coenzyme A (AcCoA) dependent acetyltransferases capable of multi-acetylating a variety of AGs[7, 9] and lysine-containing peptides such as the anti-TB drug capreomycin.[10] However the actual number of acetylations and the positions of the amines that get acetylated are highly dependent on the structure of the AG being modified (Figure 1B). Despite their high sequence (Figure 2) and structural (Figure 3A) similarities, Eis_*Mtb* and Eis_*Msm* differ in their substrate and inhibition profiles. One difference is that Eis_*Msm* is capable of di-acetylating the rigid fused-ring AG apramycin (APR, Figure 1A), whereas APR is a poorer substrate for Eis_*Mtb*.[9]

A structural examination of these two Eis homologs revealed striking differences in their AG binding pockets. The substrate binding pocket of Eis_*Mtb* is divided by Glu401 into two narrow channels (Figure 3C).[7] In contrast, because the corresponding residue in Eis_*Msm* is the much smaller Gly401, the binding pocket of Eis_*Msm* is one large, continuous cavity (Figure 3D).([11] Residues lining the AG binding pocket in Eis_*Mtb* include Ile268, Trp289, Gln291, and Glu401 (Figure 2). In Eis_*Msm*, these residues correspond to Gly266, Ala287, Ala289, and Gly401, respectively, which are all much smaller than those in Eis_*Mtb*. We previously proposed that the larger size of the AG binding cavity of Eis_*Msm* helps APR acetylation.[9] In addition, His119 (Thr119 in Eis_*Msm*), which is located in the binding pocket, was previously demonstrated to be important for acetylation activity of Eis.[7] As observed in the previously published crystal structure of Eis_*Mtb*, the position of the backbone of His119 must be critical for catalysis, as its backbone amide coordinates the catalytic water molecule to the amino group of the AG positioning it for acetylation. We previously demonstrated that mutation of His119 to Ala reduced Eis_*Mtb* activity with ten different AGs, suggesting that the side chain of His119 also plays an important role in AG binding or catalysis.[7]

To investigate the role of these five residues in AG binding, we have conducted a mutational analysis redesigning the Eis_*Mtb* active site to contain residues from Eis_*Msm*. Single mutations (H119T, I268G, W289A, Q291A, and E401G) of the residues lining the AG binding pocket were generated to explore their individual roles in AG binding and enzymatic activity. These mutations were also combined to form additional double, triple, quadruple, and quintuple Eis_*Mtb*-mutants to investigate the overall flexibility of the AG binding pocket. Initial activity profiles of the purified Eis_*Mtb*-mutants were determined with three AGs: KAN, paromomycin (PAR), and APR. The mutant-AG pairs displaying reasonable activity were further characterized to determine their Michaelis-Menten kinetic constants. Interpreting these results within the context of the Eis structure reveals important properties governing AG binding to Eis.

MATERIALS AND METHODS

Bacterial Strains, Plasmids, Materials, and Instrumentation

All chemicals, including dithionitrobenzoic acid (DTNB), AcCoA, APR, and KAN were purchased from Sigma-Aldrich (Milwaukee, WI), with the exception of PAR, which was purchased from AK Scientific (Mountain View, CA). The pH of buffers was adjusted at rt. Chemically competent *Escherichia coli* TOP10 and BL21(DE3) strains were purchased from Invitrogen (Carlsbad, CA). The pET28a plasmid used for cloning experiments was purchased from Novagen (Gibbstown, NJ). PCR primers were purchased from Integrated DNA Technologies (Coralville, IA). Restriction enzymes, Phusion DNA polymerase, T4 DNA ligase, and all other cloning reagents were purchased from New England Biolabs (Ipswich, MA). Spectrophotometric assays were performed in 96-well plates using a multimode SpectraMax M5 plate reader from Molecular Devices (Sunnyvale, CA). Liquid chromatography mass spectrometry (LCMS) was performed on a Shimadzu LCMS-2019EV composed of a LC-20AD liquid chromatograph and a SPD-20AV UV-Vis detector. The PDB structures 3R1K (Eis_*Mtb*)[7] and 3SXN (Eis_*Msm*)[11] were visualized using PyMOL (The PyMOL Molecular Graphics System, Version 1.5.0.4, Schrödinger, LLC).

Preparation of Eis_*Mtb* -Mutant Constructs by Site-Directed Mutagenesis

The splicing by overlap extension (SOE) method[12] was used to create all single (H119T, I268G, W289A, Q291A, and E401G, abbreviated as H, I, W, Q, and E mutants respectively), double (HI, HE, IW, IE, WQ, and WE), triple (HIW, HIE, HWQ, IWQ, and WQE), quadruple (HIWE and HWQE), and quintuple (HIWQE) Eis_*Mtb*-mutant constructs. The primers used for amplification of the *eis-Mtb*-mutant gene sequences are listed in Tables S1 and S2 of the Supporting Information. The H, I, W, Q, and E single mutants and the WQ double mutant were first constructed using pEis_*Mtb*-pET28a that we previously generated[7] as a template. In the first round of PCR, the gene fragments upstream and downstream of the mutation(s) were individually amplified in two separate reactions: (1) using the 5' primer for *eis_Mtb-wt* with the 3' primer for the *mutant*, and (2) using the 5' primer for the *mutant* with the 3' primer for *eis_Mtb-wt*, respectively (Table S1). After gel purification, the resulting pairs of PCR fragments were combined and used as templates for the second round of PCR amplification using the 5' and 3' primers for *eis_Mtb-wt* (Table S1). A pET28a vector, linearized at the *Nde*I and *Bam*HI restriction sites, was used for insertion of the digested complete mutant PCR products to generate the plasmids used for overexpression and protein purification. The double, triple, quadruple, and quintuple mutants were constructed similarly using the single, double, triple, and quadruple mutants as templates, respectively. The construction of all 19 mutants is summarized in Table S2 of the Supporting Information. The Eis_*Mtb*-mutant-containing plasmids were transformed into *E. coli* TOP10 cells. The *eis_Mtb*-mutant sequences were confirmed by DNA sequencing (University of Michigan DNA Sequencing Core) and comparison with the *eis_Mtb-wt* sequence (gene locus *Rv2416c*).

Overexpression and Purification of Eis_*Mtb*-Mutants

Eis_*Mtb*-mutants containing an N-terminal His_6-tag were overexpressed in *E. coli* BL21(DE3) and purified by using Ni^{II}-NTA agarose resin (Qiagen) following the procedure that we previously described for the Eis_*Mtb*[7] and Eis_*Msm*.[9] Fractions containing the desired Eis_*Mtb*-mutant proteins, as determined by SDS-PAGE, were pooled, dialyzed into Tris-HCl (50 mM, pH 8.0) overnight, and stored at 4 °C where they retained activity for at least one month. Yields of purified Eis_*Mtb*, Eis_*Msm*, and Eis_*Mtb*-mutants (Table S3) and their purities (Figure S1) are reported in the Supporting Information.

Determination of Eis_*Mtb*-Mutant Activity with KAN, PAR, and APR by Spectrophotometric Assay

Ellman's reagent was used to determine the acetyltransferase activity of all 19 Eis_*Mtb*-mutants with KAN, PAR, and APR. Briefly, the thiol group of the released CoA reacted with DTNB and the increase in absorbance (ε_{412} = 14,150 $M^{-1}cm^{-1}$)[13] was monitored at 412 nm. The addition of Eis_*Mtb*-mutant (0.5 μM) initiated reactions (200 μL) containing the AGs (APR, KAN, or PAR, 0.1 mM, 1 eq), AcCoA (0.5 mM, 5 eq), and DTNB (2 mM) in Tris-HCl (50 mM, pH 8.0). Absorbance values were recorded every 30 s for 1 h in 96-well plates, maintained at 25 °C. To confirm that the Eis_*Mtb*-mutants generated did not hydrolyze AcCoA on their own, controls in the absence of AGs were done for all mutants. No significant cleavage of AcCoA was observed in the absence of AGs.

Determination of Eis_*Mtb*-Mutants Steady-state Kinetic Parameters

Reactions (200 μL) contained a fixed AcCoA concentration (0.5 mM) and AG (KAN, PAR, APR) concentrations of 0, 20, 50, 100, 250, 500, 1000, and 2000 μM. Initiation of reaction mixtures containing DTNB (2 mM), Tris-HCl (50 mM, pH 8.0), and Eis_*Mtb*-mutants (0.25 μM for assays with KAN and PAR; 1 μM for assays with APR) was accomplished through the addition of the AG. Assays were performed in triplicate. Absorbance values were recorded at 412 nm every 20 s for 20 min at 25 °C. A non-linear regression fit to the Michaelis-Menten equation was performed using Sigma Plot 11.0 software (Systat Software Inc.; San Jose, CA) to determine the K_m and k_{cat} parameters (Table 1 and Figures S2–S4 of the Supporting Information).

Determination of Degree of Acetylation by Eis_*Mtb*-Mutants

Reactions (30 μL) containing PAR (0.67 mM), AcCoA (3.35 mM), Eis enzyme (5 μM), and Tris-HCl (50 mM, pH 8.0) were incubated overnight at rt. Reactions were quenched by addition of ice-cold methanol (30 μL) and kept at −20 °C for at least 20 min. To remove excess enzyme from the solution, the reaction mixtures were centrifuged (13,000 rpm, 10 min, rt) and diluted with H_2O (60 μL) prior to loading onto the LCMS. Samples were run using H_2O (0.1% formic acid). All mass spectra are presented in Figure S5.

Determination of Regiospecificity of Acetylation by TLC

Reactions (30 μL) containing Tris-HCl (50 mM, pH 8.0), Eis enzyme (5 μM), AcCoA (4 mM), and KAN (0.8 mM) were performed at rt. Aliquots (4 μL) were loaded onto a TLC plate (SiO_2 gel 60 F_{254} from Merck) after 0, 1, 5, 10, 30, 120 min, and overnight incubation and run using a 3:1/MeOH:NH_4OH mixture as the eluent system. The plate was dried and visualized by cerium molybdate stain (5 g CAN, 120 g ammonium molybdate, 80 mL H_2SO_4, 720 mL H_2O) (Figure S6).

RESULTS

Overexpression and Purification of Eis_*Mtb*-Mutants

Recombinant Eis_*Mtb*, Eis_*Msm*, and Eis_*Mtb*-mutants were expressed in *E. coli*, purified by Ni^{II}-NTA affinity chromatography (Figure S1 of the Supporting Information), and used in activity assays.

Determination of the Activity of Eis_*Mtb*, Eis_*Msm*, and Eis_*Mtb*-Mutants with KAN, PAR, and APR

We first characterized the activity of all Eis_*Mtb*-mutants with KAN, PAR, and APR to determine whether they retained acetyltransferase activity. The initial rates of acetylation (CoA release) by the Eis_*Mtb*-mutants with KAN, PAR, and APR were calculated and for

Eis_*Mtb*-mutant:AG combinations with initial rates at or above 10.5 nM/s, we additionally performed the Michaelis-Menten analysis of the initial reaction rate as a function of concentration of AG (Table 1).

Activity of Wild-type Eis_*Mtb* and Eis_*Msm*

Overall, the initial acetylation rates for Eis_*Msm* with KAN (41 nM/s) and PAR (22 nM/s) were much faster than with APR (2.7 nM/s). Because of the significantly lower activity of Eis_*Msm* with APR, and the fact that only Eis_*Mtb*-W289A had detectable activity, results with APR will be reported later in this section. Relative to Eis_*Mtb*, Eis_*Msm* displayed a considerably higher initial rate with PAR and a higher initial rate with KAN. As previously reported, the K_m values for the AGs are lower for both KAN and PAR with wild-type Eis_*Mtb* (K_m = 330 μM and 110 μM, respectively) than for wild-type Eis_*Msm* with KAN and PAR (K_m = 665 μM and 738 μM, respectively) (Table 1).[14] The difference in binding affinities between these two Eis isoforms reflected by these values may result from changes in AG binding pocket size and the ability of the residues lining this pocket to interact with the AGs. We tested this hypothesis by analyzing the effects of single and multiple mutations within the AG binding pocket of Eis_*Mtb* (Figure 3).

Activity of Eis_*Mtb* Single Mutants with KAN and PAR

All of the Eis_*Mtb*-mutants examined here, in which residues within Eis_*Mtb* were mutated to the corresponding Eis_*Msm* residues, had weaker observed AG binding affinities (higher K_m values) than that of wild-type Eis_*Mtb* ($K_{m,KAN}$ = 330 μM, $K_{m,PAR}$ = 110 μM). Mutations of individual Eis_*Mtb* to Eis_*Msm* residues gave mixed results with respect to catalytic efficiencies (Figure 4). Converting His119, Ile268, and Trp289 of Eis_*Mtb* to Thr, Gly, and Ala, respectively, significantly perturbed the catalytic efficiencies of KAN and PAR acetylation. However, mutating Gln291 to Ala resulted in an increase in the reaction efficiency of KAN acetylation, but significantly decreased that of PAR acetylation when compared to Eis_*Mtb* (Figure 4). The most noticeable kinetic difference observed with the single Eis_*Mtb*-mutants was the increased k_{cat} of Eis_*Mtb*-Q291A with KAN (k_{cat} = 1.08 s^{-1}), which was twice as high as the catalytic turnover determined for wild-type Eis_*Mtb* with KAN (k_{cat} = 0.53 s^{-1}) and nearly three times as high as that established for wild-type Eis_*Msm* with KAN (k_{cat} = 0.36 s^{-1}). For all single mutants, a decrease in catalytic turnover with PAR was observed as indicated by a k_{cat} value lower than that for Eis_*Mtb* (k_{cat} = 0.14 s^{-1}). For both KAN and PAR, the Eis_*Mtb*-E401G mutant displayed dramatically reduced activity when compared to Eis_*Mtb* (Figure 4), as evidenced by its poor catalytic efficiency for KAN (k_{cat}/K_m = 107 $M^{-1}s^{-1}$) (Table 1).

Activity of Eis_*Mtb* Multiple Point Mutants with KAN and PAR

Combinations of all mutations resulted in decreased catalytic efficiency with respect to wild-type Eis_*Mtb* and catalytic efficiencies were even lower than those observed for Eis_*Msm*, with the exception of Eis_*Mtb*-W289A/Q291A where the catalytic efficiency of KAN acetylation was roughly equal to that of Eis_*Msm* (Figure 4). Interestingly the triple mutant Eis_*Mtb*-I268G/W289A/Q291A also retained catalytic efficiency of KAN acetylation equal to that of Eis_*Msm*. In the case of PAR, these two favorable multiple point mutants (W289A/Q291A and I268G/W289A/Q291A) also displayed noticeably higher catalytic efficiencies than any of the other multiple mutants generated, albeit somewhat lower than that of Eis_*Msm*. All multiple point mutants bearing the unfavorable single mutation E401G displayed poor overall activity with KAN and PAR. Aside from these general trends among the mutants studied with KAN and PAR, there were some outlying results observed (*e.g.*, the double mutant W289A/E401G displayed catalytic efficiencies superior to that of the single E401G mutant with both KAN and PAR) (Figure 4).

Determination of Degree and Regiospecificity of Acetylation by Eis_*Mtb*-Mutants

To establish if the extent of acetylation (mono-, di-, or tri-) of the AG substrates is affected by single point and multiple point mutagenesis, we performed mass spectrometric analysis of enzymatic acetylation of PAR with all of the mutants generated. We found that with Eis_*Mtb*, Eis_*Msm*, and all Eis_*Mtb*-mutants, PAR was always tri-acetylated. Figure S5 displays representative mass spectra of tri-acetylation of PAR by Eis_*Mtb*, Eis_*Msm*, Eis_*Mtb*-I268G, Eis_*Mtb*-I268G/W289A, and Eis_*Mtb*-I268G/W289A/Q291A. We also established by TLC time course that mutagenesis did not affect the extent or regiospecificity of acetylation of KAN, which was always di-acetyalted in the same order (Figure S6). All reactions revealed small amounts of mono-acetyl-KAN, with an identical R_f value of 0.26 in the first minute of reaction, with the di-acetyl-KAN (R_f 0.39) forming within 5 minutes. All reactions appeared to be complete after 30 minutes.

Activity of Eis_*Mtb*-Mutants with APR

The initial rates of acetylation of APR by Eis_*Mtb*-mutants were compared to that of Eis_*Msm* (Figure 4C). Eis_*Msm* acetylates APR much less efficiently than it does KAN or PAR. These measurements are consistent with previously reported k_{cat} values that are an order of magnitude lower for Eis_*Msm* with APR than with KAN or PAR: $k_{cat,KAN}$ = 0.36 s^{-1}, $k_{cat,PAR}$ = 0.24 s^{-1}, and $k_{cat,APR}$ = 0.019 s^{-1}.[14] One single mutant, Eis_*Mtb*-W289A, caused Eis_*Mtb* to behave similarly to Eis_*Msm*: it demonstrated significant APR acetylation activity. The APR acetylation catalytic efficiency of Eis_*Mtb*-W289A was 20% of that of Eis_*Msm*. The binding affinity for APR to Eis_*Mtb*-W289A (K_m = 195 μM) was similar to that of Eis_*Msm* (K_m = 150 μM), while the k_{cat} value was four-fold smaller (0.019 s^{-1} for Eis_*Msm* and 0.005 s^{-1} for Eis_*Mtb*-W289A) (Table 1).

DISCUSSION

Because of its prominent role in bacterial resistance, a better understanding of the activity of the Eis protein is needed. We recently reported the substrate and multi-acetylation profiles of Eis_*Mtb* and Eis_*Msm*, demonstrating the unique multi-acetylation capabilities of Eis enzymes.[7, 9, 10] Eis is overall hexameric, featuring tripartite monomers containing an N-terminal and central GCN5 *N*-acetyltransferase (GNAT) regions; only the N-terminal GNAT region has catalytic residues (Tyr126 and the C-terminal carboxylate) and binds AcCoA. The overall structures of Eis proteins from these two mycobacteria are very similar, but the differences include a few important residues in the substrate binding pockets (Figures 2 and 3). The residues in Eis_*Mtb* tend to be bulkier than those of Eis_*Msm* leading to different sized and shaped AG binding pockets (Figure 3); the more open, large cavity of Eis_*Msm* has been proposed to better accommodate larger and/or conformationally constrained AGs.[9]

Redesigning and expanding the substrate specificity profile of enzymes is a topic of interest for many research groups.[15–20] In this study, we performed site-specific mutational studies for the following reasons: (i) to explore if we could redesign AG specificity of Eis_*Mtb*, (ii) to better understand which residues of Eis_*Mtb* play an important role in conferring resistance to AGs, (iii) to investigate if we could alter the regiospecificity and/or the number of sites acetylated by Eis_*Mtb*-mutants for future chemoenzymatic formation of novel AGs, and (iv) to potentially gain insight into the mechanism of action of Eis enzymes. We made mutations of five bulky residues that form the AG binding pocket in Eis_*Mtb* to the corresponding smaller residues in Eis_*Msm*. These mutations are expected to increase the size of the AG binding pocket of Eis_*Mtb* to resemble that of Eis_*Msm* (Figure 3). We chose three AGs for these studies: KAN, PAR, and APR (Figure 1A). KAN was chosen because of its immediate relevance to TB; KAN-resistance in XDR-*Mtb* clinical isolates

results from *eis* upregulation.[4] PAR and APR were selected for investigation because they represent additional diverse structural scaffolds; KAN contains a 4,6-substituted-2-deoxystreptamine (4,6-DOS) ring, while PAR contains a 4,5-DOS ring with an additional sugar moiety (ring IV). With two of its four rings fused, APR represents a third unique rigid AG scaffold. Additionally, APR is a substrate of Eis_*Msm*, whereas it is a very poor substrate of Eis_*Mtb*.

Effects of Single Mutations on Eis_*Mtb* Activity with KAN and PAR

To gain insight into the role of His119, Ile268, Trp289, Gln291, and Glu401 in Eis_*Mtb* activity and AG binding, we first converted these residues into their corresponding residues in Eis_*Msm* (Figures 2 and 3). Of individual mutations of the three residues (I268G, W289A, and Q291A) lining one side of channel 2 in the Eis_*Mtb* AG binding pocket (Figure 3), only Q291A increased catalytic efficiency when compared to that of the wild-type Eis_*Mtb* with KAN. Moreover, Eis_*Mtb*-I268G and Q291A mutants had higher efficiency with KAN than Eis_*Msm* did. The Q291A mutation led to a dramatic increase in KAN acetylation activity in Eis_*Mtb* as evidenced by a higher k_{cat} value (1.08 s^{-1}) in comparison with Eis_*Msm* (k_{cat} = 0.36 s^{-1}). As hypothesized, the individual I268G and W289A mutations made Eis_*Mtb* behave more like Eis_*Msm*. Mechanistically, this observed decrease in activity may be explained as follows: a larger cavity may not bind AGs as well as a narrower one, consistent with the higher K_m values observed for Eis_*Msm* and Eis_*Mtb*-mutants than for wild-type Eis_*Mtb*.

The Eis_*Mtb*-E401G mutant showed a dramatic decrease in catalytic efficiency with both KAN and PAR when compared to either Eis_*Mtb* or Eis_*Msm*. Glu401 is the penultimate residue of the protein C-terminus and is flanked by the C-terminal residue Phe402. The buried side chain of Phe402 points towards the protein interior, positioning the terminal carboxyl group to act as a catalytic base during acetylation. Mutating Glu401 to a flexible Gly may increase the backbone flexibility that is compensated in the context of Eis_*Msm* residues, but not in Eis_*Mtb*, possibly disturbing the position of the terminal carboxyl group. Previous studies found that Eis with a C-terminal His_6-tag as well as a truncated version (Eis_*Mtb* 1–399) eliminated nearly all acetylation activity, further highlighting the importance of this C-terminal region.[7]

With KAN, Eis_*Mtb*-H119T maintained activity similar to that of Eis_*Msm*. However, with PAR, Eis_*Mtb*-H119T showed a significant decrease in efficiency compared to both wild-type Eis_*Mtb* and Eis_*Msm*. These results, in combination with the fact that Eis_*Mtb*-H119A displays very poor activity with KAN and PAR,[7] indicate that a polar amino acid residue or a residue that can donate or accept hydrogen bonds may be required at that position in the Eis active site.

Effects of Multiple Mutations on Eis_*Mtb* Activity with KAN and PAR

To determine if the divided Eis_*Mtb* active site could be progressively converted to the larger non-divided Eis_*Msm* AG binding cavity, we next generated a variety of double, triple, quadruple, and quintuple Eis_*Mtb*-mutants. The most active double Eis_*Mtb*-mutant W289A/Q291A and triple mutant Eis_*Mtb*-I268G/W289A/Q291A maintained high activity with KAN equivalent to that of Eis_*Msm*, while they displayed a slight decrease in catalytic efficiency with PAR when compared to Eis_*Msm* (Figure 4). This agrees well with what was observed with the single mutants and suggests that the I268G, W289A, and Q291A mutations allow Eis_*Mtb* to become very similar in activity to Eis_*Msm*. All three of these residues line channel 2 of the AG binding site within Eis_*Mtb* (Figure 3). Mutating these residues to smaller side chains enlarges channel 2, which may help to better accommodate both KAN and PAR scaffolds with only decreasing the turnover rate to the level of

Eis_*Msm*. Generally, multiple mutations did not display a consistent additive or non-additive pattern, likely due to their interactions either directly or through the bound AGs. Consistent with the loss of activity for the single Eis_*Mtb*-E401G mutant, all multiple mutants containing the E401G mutation showed a dramatic decrease in activity with KAN and PAR.

Effects of Mutations on Degree and Regiospecificity of Acetylation

To determine the effect of mutating the five residues studied on the degree and regiospecificity of acetylation of KAN and PAR, we performed mass spectrometry and TLC experiments. By mass spectrometry, the single and multiple point Eis_*Mtb*-mutants did not result in any changes in the number of sites acetylated on PAR (Figure S5). By TLC time course, Eis_*Mtb*-mutants were found to acetylate KAN in the same order as Eis_*Mtb* and Eis_*Msm* (Figure S6). Mono-acetyl-KAN was formed during the first minute of the enzymatic reactions and di-acetyl-KAN was observed after 5 minutes with apparent completion of all di-acetylation reactions after 30 minutes. Identical R_f values for all mono-acetyl-KAN (R_f 0.26) and di-acetyl-KAN (R_f 0.39) indicated that mutation of the five residues studied do not alter the regiospecificty of the Eis enzymes.

Effects of Eis_*Mtb* Mutations on Activity with APR

The only mutant that demonstrated detectable activity with the large and rigid APR was Eis_*Mtb*-W289A. This can easily be rationalized by the considerable steric changes that this mutation causes in the AG binding pocket. Trp289 bears a very bulky indole side chain and eliminating this large group extends the depth of channel 2 in the Eis_*Mtb* active site (Figure 3), making it large enough to accommodate the long restricted structure of APR.

In summary, we have presented evidence that three of the five residues mutated, Ile268, Trp289, and Gln291 are important in controlling the efficiency of KAN and PAR acetylation. We have also demonstrated that Trp289 is an important residue for APR acetylation. Finally, we have shown that Glu401 plays a key role in the overall activity of Eis_*Mtb*. It is worth noting that out of the five mutations in this study only the Glu to Gly mutation can be achieved by a single nucleotide substitution (and would be inactivating). Therefore, resistance is not likely to evolve further through the mutations that we considered. Our lab is currently investigating Eis inhibitors for combination therapy with AGs and examining their effectiveness across a broad spectrum of mycobacterial and non-mycobacterial species containing Eis proteins. In conjunction with our previous work on the identification of inhibitors of Eis_*Mtb*,[21] the knowledge gained in the current study will aid in the design of Eis inhibitors for co-delivery with AGs to treat resistant infections.

Supplementary Material

Refer to Web version on PubMed Central for supplementary material.

Acknowledgments

This work was supported by National Institutes of Health grant AI090048 (to S.G.-T.). We thank Rachel E. Pricer for cloning and preliminary experimental work. We thank Dr. Oleg V. Tsodikov for critical reading of the manuscript and insightful comments.

Glossary

AcCoA	acetyl coenzyme A
AG	aminoglycoside

APR	apramycin
CoA	coenzyme A
DTNB	dithionitrobenzoic acid
Eis	enhanced intracellular survival
KAN	kanamycin A
MDR	multidrug-resistant
Msm	*Mycobacterium smegmatis*
Mtb	*Mycobacterium tuberculosis*
PAR	paromomycin
SDS-PAGE	sodium dodecyl sulfate-polyacrylamide gel electrophoresis
TB	tuberculosis
XDR	extensively drug-resistant

REFERENCES

1. Ellner JJ. The emergence of extensively drug-resistant tuberculosis: a global health crisis requiring new interventions: part I: the origins and nature of the problem. Clin Transl Sci. 2008; 1:249–254. [PubMed: 20443856]
2. Banerjee R, Schecter GF, Flood J, Porco TC. Extensively drug-resistant tuberculosis: new strains, new challenges. Expert Rev Anti Infect Ther. 2008; 6:713–724. [PubMed: 18847407]
3. Udwadia ZF, Amale RA, Ajbani KK, Rodrigues C. Totally drug-resistant tuberculosis in India. Clin Infect Dis. 2012; 54:579–581. [PubMed: 22190562]
4. Zaunbrecher MA, Sikes RD Jr, Metchock B, Shinnick TM, Posey JE. Overexpression of the chromosomally encoded aminoglycoside acetyltransferase eis confers kanamycin resistance in Mycobacterium tuberculosis. Proc Natl Acad Sci U S A. 2009; 106:20004–20009. [PubMed: 19906990]
5. Campbell PJ, Morlock GP, Sikes RD, Dalton TL, Metchock B, Starks AM, Hooks DP, Cowan LS, Plikaytis BB, Posey JE. Molecular detection of mutations associated with first- and second-line drug resistance compared with conventional drug susceptibility testing of Mycobacterium tuberculosis. Antimicrob Agents Chemother. 2011; 55:2032–2041. [PubMed: 21300839]
6. Jnawali HN, Yoo H, Ryoo S, Lee KJ, Kim BJ, Koh WJ, Kim CK, Kim HJ, Park YK. Molecular genetics of Mycobacterium tuberculosis resistant to aminoglycosides and cyclic peptide capreomycin antibiotics in Korea. World J Microbiol Biotechnol. 2013
7. Chen W, Biswas T, Porter VR, Tsodikov OV, Garneau-Tsodikova S. Unusual regioversatility of acetyltransferase Eis, a cause of drug resistance in XDR-TB. Proc Natl Acad Sci U S A. 2011; 108:9804–9808. [PubMed: 21628583]
8. Reyrat JM, Kahn D. Mycobacterium smegmatis: an absurd model for tuberculosis? Trends Microbiol. 2001; 9:472–474. [PubMed: 11597444]
9. Chen W, Green KD, Tsodikov OV, Garneau-Tsodikova S. Aminoglycoside multiacetylating activity of the enhanced intracellular survival protein from Mycobacterium smegmatis and its inhibition. Biochemistry. 2012; 51:4959–4967. [PubMed: 22646013]
10. Houghton JL, Green KD, Pricer RE, Mayhoub AS, Garneau-Tsodikova S. Unexpected N-acetylation of capreomycin by mycobacterial Eis enzymes. J Antimicrob Chemother. 2012
11. Kim KH, An DR, Song J, Yoon JY, Kim HS, Yoon HJ, Im HN, Kim J, Kim do J, Lee SJ, Lee HM, Kim HJ, Jo EK, Lee JY, Suh SW. Mycobacterium tuberculosis Eis protein initiates suppression of host immune responses by acetylation of DUSP16/MKP-7. Proc Natl Acad Sci U S A. 2012; 109:7729–7734. [PubMed: 22547814]

12. Ho SN, Hunt HD, Horton RM, Pullen JK, Pease LR. Site-directed mutagenesis by overlap extension using the polymerase chain reaction. Gene. 1989; 77:51–59. [PubMed: 2744487]
13. Riddles PW, Blakeley RL, Zerner B. Reassessment of Ellman's reagent. Methods Enzymol. 1983; 91:49–60. [PubMed: 6855597]
14. Pricer RE, Houghton JL, Green KD, Mayhoub AS, Garneau-Tsodikova S. Biochemical and structural analysis of aminoglycoside acetyltransferase Eis from Anabaena variabilis. Mol Biosyst. 2012; 8:3305–3313. [PubMed: 23090428]
15. Green KD, Porter VR, Zhang Y, Garneau-Tsodikova S. Redesign of cosubstrate specificity and identification of important residues for substrate binding to hChAT. Biochemistry. 2010; 49:6219–6227. [PubMed: 20560540]
16. Williams GJ, Zhang C, Thorson JS. Expanding the promiscuity of a natural-product glycosyltransferase by directed evolution. Nat Chem Biol. 2007; 3:657–662. [PubMed: 17828251]
17. Moretti R, Chang A, Peltier-Pain P, Bingman CA, Phillips GN Jr, Thorson JS. Expanding the nucleotide and sugar 1-phosphate promiscuity of nucleotidyltransferase RmlA via directed evolution. J Biol Chem. 2011; 286:13235–13243. [PubMed: 21317292]
18. Yi H, Cho KH, Cho YS, Kim K, Nierman WC, Kim HS. Twelve positions in a beta-lactamase that can expand its substrate spectrum with a single amino acid substitution. PLoS One. 2012; 7:e37585. [PubMed: 22629423]
19. Rale M, Schneider S, Sprenger GA, Samland AK, Fessner WD. Broadening deoxysugar glycodiversity: natural and engineered transaldolases unlock a complementary substrate space. Chemistry. 2011; 17:2623–2632. [PubMed: 21290439]
20. Addington T, Calisto B, Alfonso-Prieto M, Rovira C, Fita I, Planas A. Re-engineering specificity in 1,3-1, 4-beta-glucanase to accept branched xyloglucan substrates. Proteins. 2011; 79:365–375. [PubMed: 21069723]
21. Green KD, Chen W, Garneau-Tsodikova S. Identification and characterization of inhibitors of the aminoglycoside resistance acetyltransferase Eis from Mycobacterium tuberculosis. ChemMedChem. 2012; 7:73–77. [PubMed: 21898832]

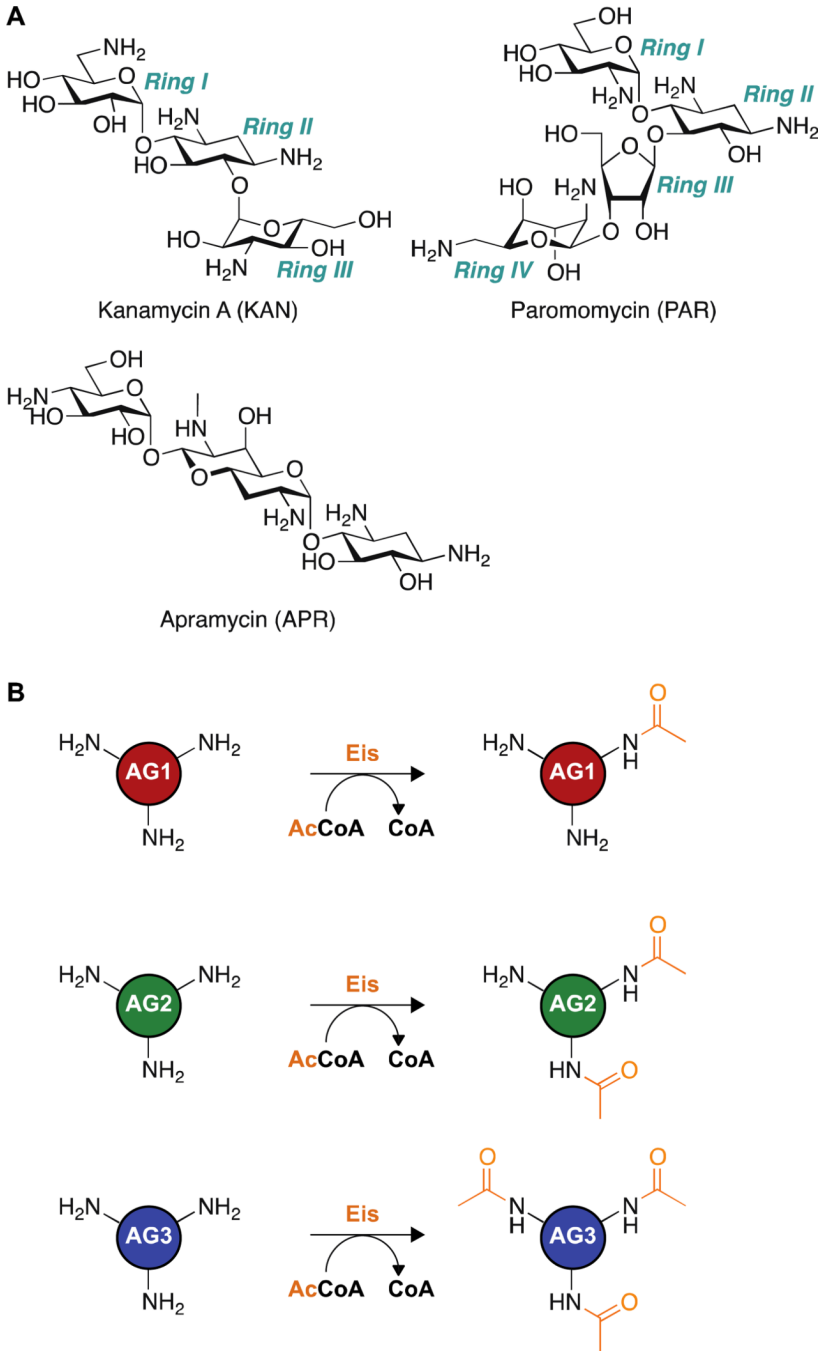

Figure 1.

A. Structures of AGs used in this study: kanamycin A (KAN), paromomycin (PAR), and apramycin (APR). **B**. Schematic of the reaction catalyzed by Eis enzymes. Eis is capable of mono-, di-, or tri-acetylating AGs, depending on the AG structure and the Eis isoform. The positions of acetylation (1, 2', and 6') by Eis_*Mtb* have, to date, only been reported for neamine.[7]

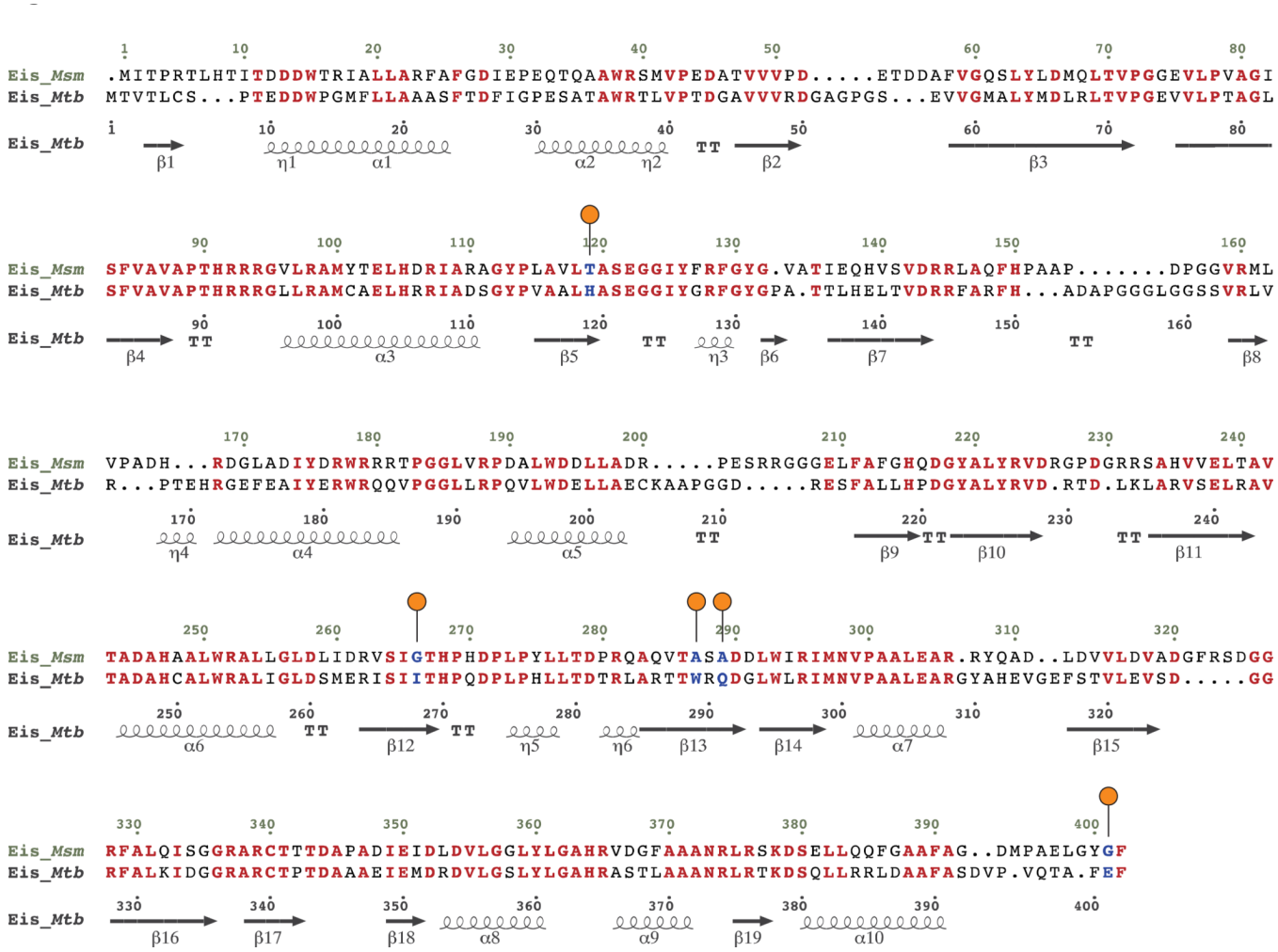

Figure 2.

Structure-based sequence alignment of Eis_*Mtb* and Eis_*Msm*. Residues in bold red are conserved between the two Eis homologs. Residues mutated in this study are in bold blue and marked with orange circles above the sequence.

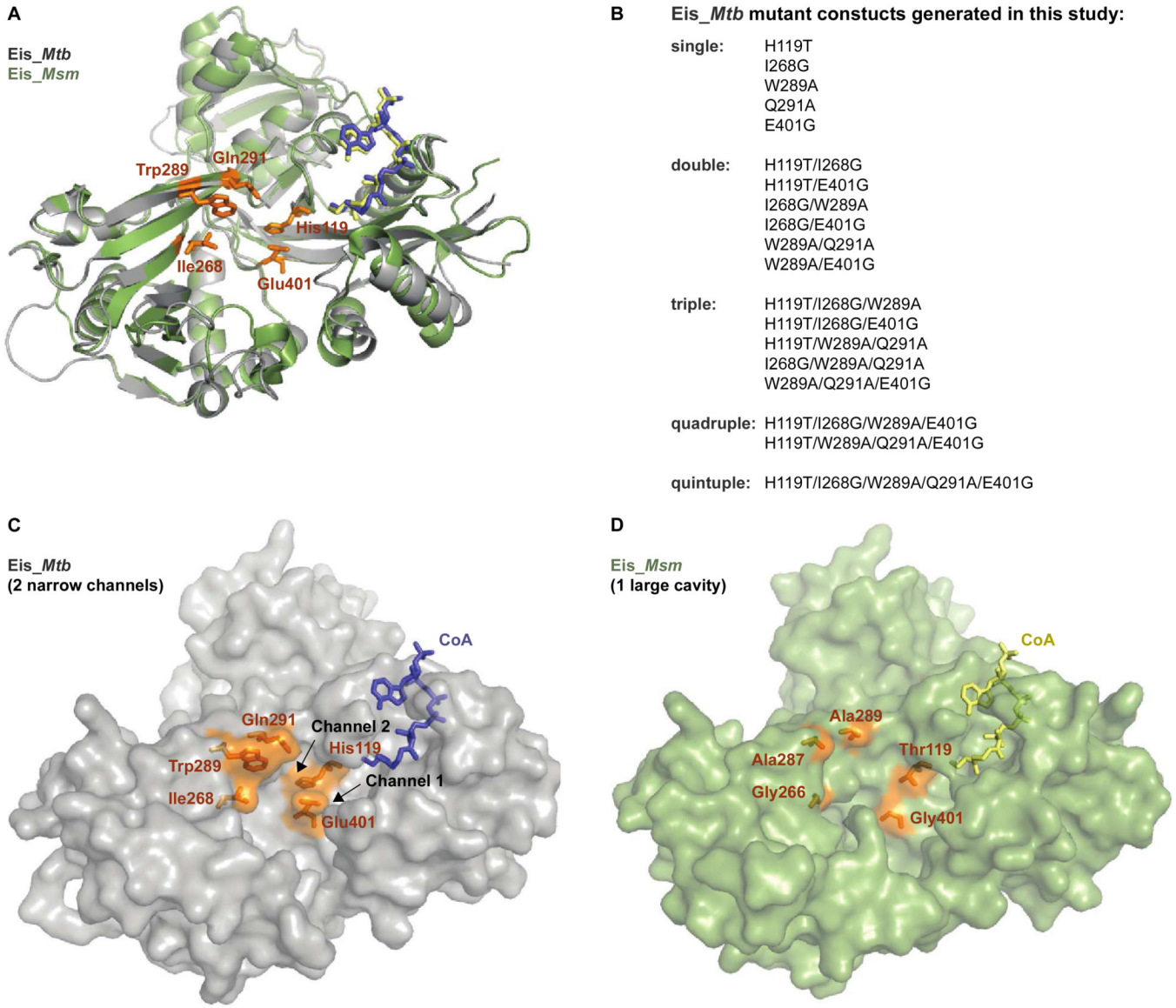

Figure 3.

Structural differences between the AG binding pockets of Eis_*Mtb* and Eis_*Msm***A**. Cartoon overlay of Eis_*Mtb* (gray; PDB code: 3R1K[(7)]) and Eis_*Msm* (green; PDB code: 3SXN[(11)]). Coenzyme A (CoA) is shown as blue (Eis_*Mtb*) or yellow (Eis_*Msm*) sticks. The five residues lining the Eis_*Mtb* AG binding pocket that were mutated in these studies are shown as orange sticks. **B**. List of Eis_*Mtb*-mutant constructs examined in this study. **C**. Surface representation of Eis_*Mtb* (gray) with CoA (blue sticks) and active site residues (orange sticks). The Eis_*Mtb* active site is divided into two narrow channels by Glu401. **D**. Surface representation of Eis_*Msm* (green) with CoA (yellow sticks) and active site residues (orange sticks) to which the Eis_*Mtb* corresponding residues were mutated.

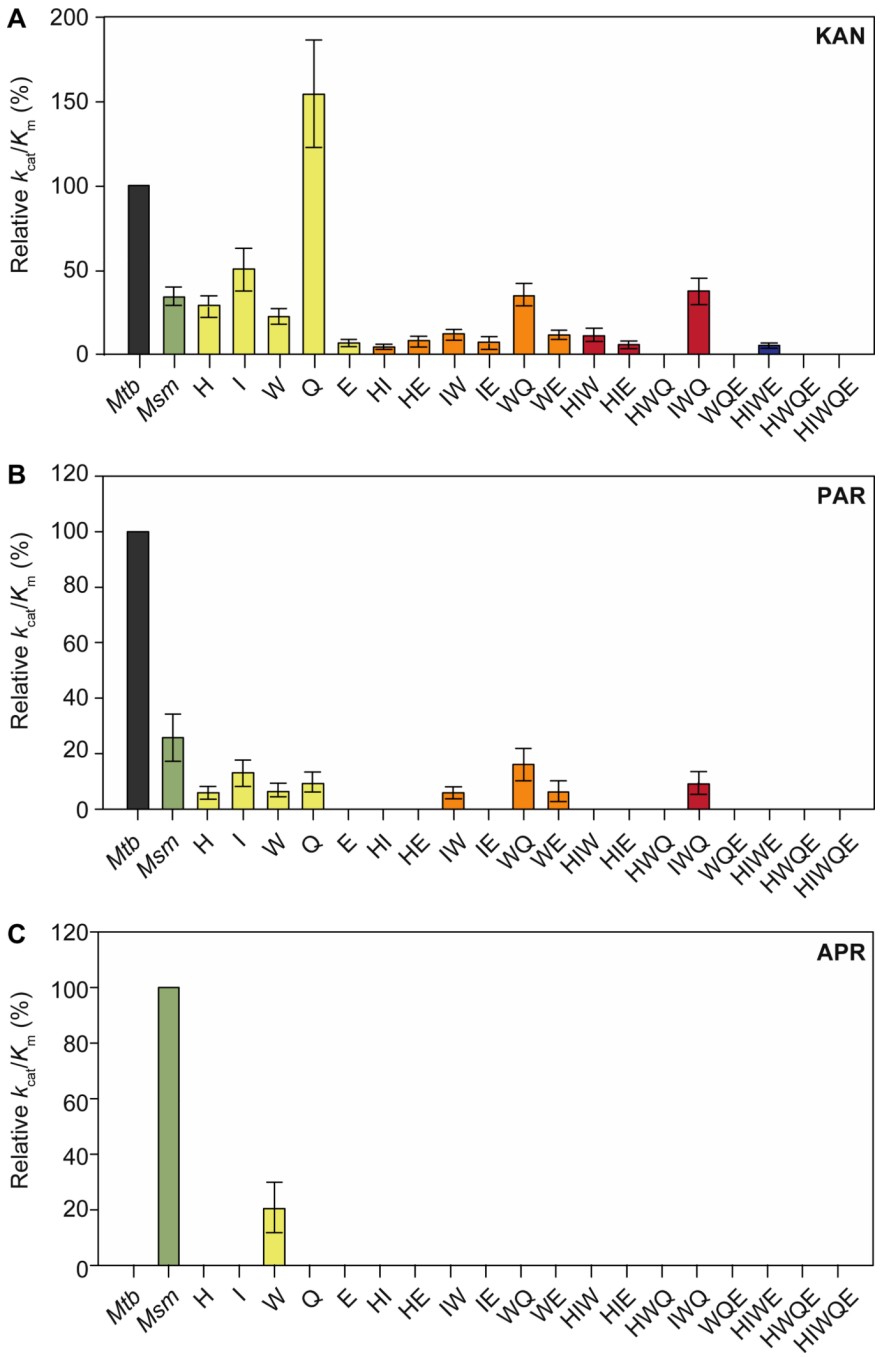

Figure 4.

Relative catalytic efficiencies (k_{cat}/K_m) for Eis_*Mtb*-mutants. **A**. Activity of Eis_*Mtb*-mutants with KAN, normalized to Eis_*Mtb*-wt (1,606 $M^{-1}s^{-1}$). **B**. Activity of Eis_*Mtb*-mutants with PAR, normalized to Eis_*Mtb*-wt (1,272 $M^{-1}s^{-1}$) **C**. Activity of Eis_*Mtb*-mutants with APR, normalized to Eis_*Msm*-wt (127 $M^{-1}s^{-1}$).

Table 1

Kinetic parameters for Eis_*Mtb*-mutants with KAN, PAR, and APR.

	KAN		
Mutant[a]	**K_m (μM)**	**k_{cat} (s^{-1})**	**k_{cat}/K_m ($M^{-1}s^{-1}$)**
Eis_*Mtb*[b]	330 ± 40	0.53 ± 0.03	1,606 ± 215
Eis_*Msm*[b]	665 ± 42	0.36 ± 0.01	541 ± 37
Eis_*Mtb*-H119T = “H”	684 ± 80	0.32 ± 0.02	468 ± 62
Eis_*Mtb*-I268G = “I”	776 ± 130	0.63 ± 0.05	812 ± 150
Eis_*Mtb*-W289A = “W”	670 ± 86	0.24 ± 0.01	358 ± 48
Eis_*Mtb*-Q291A = “Q”	438 ± 56	1.08 ± 0.05	2,465 ± 335
Eis_*Mtb*-E401G = “E”	1,397 ± 351	0.15 ± 0.02	107 ± 30
Eis_*Mtb*-H119T/I268G = “HI”	813 ± 308	0.06 ± 0.01	74 ± 31
Eis_*Mtb*-H119T/E401G = “HE”	516 ± 139	0.07 ± 0.01	135 ± 41
Eis_*Mtb*-I268G/W289A = “IW”	791 ± 112	0.15 ± 0.01	189 ± 30
Eis_*Mtb*-I268G/E401G = “IE”	908 ± 359	0.11 ± 0.02	121 ± 53
Eis_*Mtb*-W289A/Q291A = “WQ”	712 ± 86	0.40 ± 0.02	561 ± 73
Eis_*Mtb*-W289A/E401G = “WE”	679 ± 125	0.13 ± 0.01	191 ± 38
Eis_*Mtb*-H119T/I268G/W289A = “HIW”	617 ± 223	0.11 ± 0.02	178 ± 72
Eis_*Mtb*-H119T/I268G/E401G = “HIE”	673 ± 203	0.06 ± 0.01	89 ± 31
Eis_*Mtb*-H119T/W289A/Q291A = “HWQ”	--[c]	--[c]	--[c]
Eis_*Mtb*-I268G/W289A/Q291A = “IWQ”	620 ± 75	0.37 ± 0.02	597 ± 79
Eis_*Mtb*-W289A/Q291A/E401G = “WQE”	--[c]	--[c]	--[c]
Eis_*Mtb*-H119T/I268G/W289A/E401G = “HIWE”	437 ± 96	0.04 ± 0.01	92 ± 30
Eis_*Mtb*-H119T/W289A/Q291A/E401G = “HWQE”	--[c]	--[c]	--[c]
Eis_*Mtb*-H119T/I268G/W289A/Q291A/E401G = “HIWQE”	--[c]	--[c]	--[c]
	PAR		
Mutant[a]	K_m (μM)	k_{cat} (s^{-1})	k_{cat}/K_m ($M^{-1}s^{-1}$)
Eis_*Mtb*[b]	110 ± 21	0.14 ± 0.01	1,272 ± 260
Eis_*Msm*[b]	738 ± 158	0.24 ± 0.03	325 ± 81
H	643 ± 195	0.05 ± 0.01	77 ± 28
I	789 ± 194	0.13 ± 0.01	165 ± 35
W	615 ± 244	0.05 ± 0.01	81 ± 36
Q	1,019 ± 358	0.12 ± 0.02	118 ± 46
IW	1,005 ± 285	0.07 ± 0.01	70 ± 22
WQ	280 ± 77	0.06 ± 0.01	214 ± 69
WE	486 ± 271	0.04 ± 0.01	82 ± 50

	KAN		
Mutant[a]	**K_m (μM)**	**k_{cat} (s^{-1})**	**k_{cat}/K_m ($M^{-1}s^{-1}$)**
IWQ	452 ± 178	0.05 ± 0.01	111 ± 49
	APR		
Mutant[a]	K_m (μM)	k_{cat} (s^{-1})	k_{cat}/K_m ($M^{-1}s^{-1}$)
Eis_*Mtb*	×[d]	×[d]	×[d]
Eis_*Msm*[b]	150 ± 43	0.019 ± 0.002	127 ± 39
W	195 ± 64	0.005 ± 0.001	26 ± 9

[a] The abbreviations for Eis_*Mtb*-mutants are based on the amino acid residues of Eis_*Mtb* that were mutated to the corresponding residues from Eis_*Msm*. These abbreviations are used in Figure 4.

[b] These values have been previously reported and are used for comparison in this manuscript.(14)

[c] For KAN: Kinetic parameters could not be determined for the following mutants because the activity was less than 26% of the initial rate of Eis_*Mtb* with KAN (10.5 nM CoA s^{-1}, Figure 4A): HWQ, WQE, HWQE, and HIWQE. For PAR: Kinetic parameters could not be determined for the following mutants because the activity was less than 50% of the initial rate of Eis_*Mtb* with PAR (10.5 nM CoA s^{-1}, Figure 4B): E, HI, HE, IE, HIW, HWQ, WQE, HIWE, HWQE, and HIWQE. For APR: Kinetic parameters could only be determined for the W mutant with APR because the activity of all others was too low to be determined (Figure 4C).

[d] × indicates that APR is not a substrate of Eis_*Mtb*.